Synthesis and enhanced electron field emission of vertically aligned carbon nanotubes grown on stainless steel substrate

Suman Neupane, Yuehai Yang, Wenzhi Li*
Department of Physics, Florida International University, Miami, FL 33199, USA
Yihua Gao
Wuhan National Laboratory for Optoelectronics-School of Physics, Huazhong University of Science and Technology, Wuhan 430074, China

Abstract

Vertically aligned carbon nanotube (CNT) array was synthesized on pristine stainless steel (SS) substrate, chemically etched SS substrate, and Ni/Cr layer coated SS substrate via plasma enhanced chemical vapor deposition method. The effect of chemical etching on the surface morphology of the SS substrates and the growth of the CNTs were investigated. SS substrate chemically etched for 40 min resulted in CNTs with uniform diameter and length. Electron field emission properties of CNT arrays synthesized on pristine SS and Ni/Cr coated SS substrates were measured. It is found that CNTs synthesized on pristine SS substrate exhibited lower turn-on electric field, lower threshold electric field, and a higher field enhancement factor as compared to that from the CNTs synthesized on Ni/Cr coated SS. However, the CNTs synthesized on Ni/Cr coated SS showed better emission stability, which was attributed to the improved adhesion between the CNTs and SS substrate via the Cr thin layer. The results indicate that the conductive substrate, robust contact between the CNTs and the substrate, and the high stability will benefit the field emission applications of the CNTs.

* Corresponding author: Wenzhi.Li@fiu.edu, fax: (+1) 305-348-6700.

1. Introduction

Carbon nanotubes (CNTs) have attracted a great research interest since the landmark report on the discovery of CNTs by Iijima in 1991 [1]. CNTs exhibit superior chemical stability, remarkable electrical and thermal conductivities, and robust structural integrity. These properties can be exploited for possible applications in field emission devices, gas sensors, Li-ion battery, and nanoelectronics [2-4]. However, for a viable application, it is desirable to have a controlled growth of aligned CNTs at relatively lower temperatures compatible with currently available device fabrication techniques. Lately, plasma enhanced chemical vapor deposition (PECVD) process has been adopted as a suitable method to synthesize arrays of vertically aligned CNTs (VACNTs) at lower temperatures than the conventional arc-discharge or laser ablation methods [5]. In addition, it is also possible to control the length, diameter, and density of CNTs by adjusting the various parameters during the PECVD synthesis [6, 7].

CNTs are ideal candidates for electron field emission applications due to their high aspect-ratio. The emission current from CNTs can be expressed by Fowler-Nordheim (F-N) equation: $J = (A\beta^2F^2/\phi) \exp [-B\phi^{3/2}/(\beta F)]$ ……(i)

where the constants *A* and *B* are dependent on the work-function of the material and the local electric field at the emission tip [2, 7]. The effective electric field (F_{eff}) can be expressed as $F_{eff} = \beta F_o$, where F_o is the applied electric field between the CNT emitters and the anode, and β is the field enhancement factor. The large aspect-ratio of CNTs enables a higher field enhancement and consequently an increased emission current. However, for a reliable performance of a fabricated CNT emission device, the adhesion of the CNTs to the substrate and the density of the CNTs play a crucial role during the electrical measurements.

Recently, many efforts have been focused on the synthesis of arrays of VACNTs directly on conductive metals or their alloys such as copper, nickel, titanium, stainless steel (SS), inconel, nichrome and others [8-11]. The in-situ synthesis of CNTs on conductive substrates prevents the introduction of impurities and defects on CNTs incurred during the device fabrication for various applications. Growth of CNTs on metallic substrates or their alloys have been performed by first depositing a thin layer of catalyst on the metallic substrate and then initiating a thermal decomposition of carbonaceous precursor on the catalyst 'seed'. In this approach, usually the substrates were subjected to chemical or thermal treatment prior to the introduction of a carbon source for CNT growth [12-18]. Wang et al. used acid-assisted electrochemical polishing and plasma pre-treatment to obtain VACNTs on SS [12]. Park et al. treated SS substrate with HF etching and hydrogen plasma during the sequential combination of PECVD and thermal CVD to obtain randomly oriented spaghetti-like CNTs [13]. Lin et al. were successful in synthesizing CNTs on SS by microwave-PECVD and studying their field emission properties [14]. Sparse but well-aligned CNTs were synthesized for the growth period of 5 min, and the growth had to be prolonged for about 30 min to obtain a dense array of VACNTs. Synthesis of CNTs with non-uniform substrate coverage were reported by Masarapu et al. and Baddour et al. on SS substrates subjected to chemical etching to activate nucleation sites prior to the growth [15, 16]. Parthangal et al. reported the synthesis of randomly oriented and weakly adhered CNTs on SS by CVD method [11]. There have been further attempts to deposit a catalyst layer to enhance the quality of as-synthesized CNTs on SS. Abad et al. reported the PECVD synthesis of sparse and thick bundles of CNTs on bare SS as well as dense VACNTs on cobalt nanoparticles deposited on SS [17]. Kim et al. used a water assisted CVD to grow CNTs on Al and Fe coated SS [18]. Duy et al. synthesized VACNTs on Ni coated SS substrates (with a buffer layer of 100 nm TiN) by

PECVD and studied their field emission properties [10]. Most of the reported results rely on chemical, thermal, or plasma treatment of pristine SS or metal-catalyzed SS to develop active nucleation sites before the introduction of carbon precursor for the growth of CNTs. The pretreatment of substrate is regarded as an efficient and essential approach for the formation of homogenous granular nanoscale structures which act as catalysts for the uniform growth of VACNTs.

In this study, VACNT arrays were synthesized on pristine SS 304 substrate, chemically treated SS 304 substrate, and Ni/Cr thin film coated SS 304 substrate. The effect of chemical etching on the surface morphology of the SS substrates and the growth of the VACNTs on the etched SS substrates were investigated. Furthermore, the field emission performance of the VACNTs synthesized directly on SS pristine substrate and Ni/Cr coated SS substrate was evaluated to reveal the effect of the substrates on the field emission properties.

Experimental methods

VACNT arrays were synthesized by PECVD process. The details of the process have been described elsewhere [7]. Briefly, a SS substrate (1 cm × 1 cm × 0.1 mm) was loaded into a PECVD system which was then pumped to a pressure of 5×10^{-6} torr. The SS substrate was heated to a temperature of 600 °C while NH_3 was introduced at a constant flow rate of 100 sccm. Then, C_2H_2 was introduced as the carbon source at 30 sccm and the flow rate of NH_3 was maintained at 100 sccm during the entire synthesis period. The power of the DC plasma was maintained at 70 W and the pressure was maintained at 8 torr during the CNT growth. The SS substrate is type 304 stainless steel foil. Three types of SS substrates were used to grow CNTs, they were (1) pristine SS substrate, (2) Nr/Cr thin film coated SS substrate where Ni acted as a

catalyst for the growth of CNTs and Cr was a buffer layer to improve the adhesion of CNTs to the substrate and, and (3) chemically etched SS substrate. Thin Cr and Ni layers were deposited onto SS substrates by electron beam evaporation at a pressure of 2×10^{-6} torr at room temperature. The thickness of the Cr and Ni layers was 15 nm and 6.5 nm, respectively. The chemically etched SS substrates were prepared by etching the pristine SS substrates in a mixture of concentrated H_2SO_4: H_2O_2: H_2O (4: 1: 15, volume ratio) for different time durations in an ultrasonic bath.

A field emission scanning electron microscope (SEM, JEOL JSM-6330F) operated at an accelerating voltage of 15 KV was used for the surface morphology analysis. To measure the actual length of the CNTs, a scratch on the forest of the aligned CNTs was made using tweezers to result some CNTs lying on the surface. Transmission electron microscopy (TEM) images, high resolution TEM (HRTEM) images, and selected area diffraction (SAED) patterns were obtained from a JEOL-2100F apparatus operated at an accelerating voltage of 200 KV. For the TEM analysis, the CNTs synthesized on the SS substrate were removed and dispersed ultrasonically in ethanol and the solution was dropped on the carbon coated copper TEM grid. Tapping mode atomic force microscopy (AFM) images of the SS surface were acquired by Veeco Multimode Nanoscope III D. The spring constant of the Si tip was 42 N/m and the resonance frequency was between 250 and 300 kHz. The software used to analyze the surface roughness was Nanoscope Control. The field emission measurements of the CNTs were performed using a diode configuration inside a chamber at a residual pressure of 8×10^{-7} torr [19]. The emission current from CNT emitters was measured by a Keithley 4200-SCS with the electrodes maintained at 400 μm apart. The power was provided by a DC power supply (Matsusada AU-15P20).

3 Results and discussions

3.1 Effect of synthesis time on the formation of CNTs

The synthesis time plays an important role in the length and diameter of CNTs. Figs. 1(a-c) show the SEM images of CNTs synthesized on pristine SS substrates. The ammonia-plasma will etch the surface of the SS substrate resulting in small bumps, which can act as catalyst dots for growing CNTs. As evident from the growth after 3 min, the CNTs show a random distribution in the initial phase of growth. These CNTs acquire an average length of 600 nm after the 3 min growth and the diameters also differ on an individual basis. In addition to these CNTs, the substrate contains catalyst particles of irregular sizes as shown by the dark arrows in the inset. With the onset of plasma treatment, the substrate forms catalyst fragments of different dimensions; the smaller of which contribute toward the growth of the CNTs while the bigger ones remain. In comparison to the sample after 3 min growth, the CNTs after 10 min growth exhibit an increased density and length, see Fig. 1(b). After a prolonged synthesis time, new nucleation sites develop in the area where the density of the CNTs from 3 min growth was low; as a result, the density of the CNTs after 10 min will increase significantly. After 10 min growth, the average length of the CNTs is 3.4 μm with the diameter around 80 nm. It is also observed that the big catalyst particles have disappeared most probably due to the continuous etching of the plasma. The small individual catalyst particles formed from further plasma etching can initiate the growth of CNTs, contributing to an increased density of the CNTs as compared to samples with 3 min growth. A further increase in the synthesis time to 20 min leads to short and stubby microstructures with an average length of 2.5 μm and diameter of 1 μm, see Fig.1(c). It has been reported that the catalyst particles lose their catalytic activity in PECVD growth after a certain period, and then the growth of CNTs will be ceased [20]. Beyond this point, the plasma

starts the destructive etching to the CNTs which results in the taller CNTs to fall apart. These results indicate that the growth time significantly affects the length and density of the CNTs.

3.2 Effect of chemical etching on the formation of CNTs

SS 304 is commercially available with a Cr rich passive oxide film which protects against the corrosion [15]. Chemical etching of SS substrates before growth will remove this layer and expose islands of Fe which act as catalyst islands for the growth of CNTs. Figures 2(a-e) show the AFM images of the surfaces of the as-received pristine SS and the SS substrates after chemical etching for 10, 20, 40, and 60 min, respectively. As expected, the pristine SS surface is rough with grain sizes of non-uniform dimensions scattered across the surface as shown in Fig. 2(a). After etching the SS for 10 min, the surface morphology changed with the appearance of smaller particles as shown in Fig. 2(b). The density of the particles increased further after etching for 20 min, see Fig. 2(c). After 40 min, as shown in Fig. 2(d), relatively uniformly distributed fine particles were observed on the surface. However, a 60 min chemical etching resulted in ridges or lines of big particles on the substrate surface; this result is contrary to intuition. It is not clear at the moment why the ridges are formed after a 60 min chemical etching. Further work is needed to get a better understanding on this phenomenon. The root mean square roughness were 5.9, 1.8, 1.6, 1.4, and 3.6 nm for surfaces etched for 0, 10, 20, 40, and 60 min, respectively. The evolution of the surface roughness for different etching periods has been shown in Fig. 2(f). The results show that 40-minute chemical etching resulted in fine particles with uniform sizes which will be favorable for the growth of CNTs with uniform diameter. It should also be noted that very small catalyst particles may not survive the substrate treatment and CNT synthesis process, in other words, very small catalyst particles may not be able to grow CNTs.

Figures 3(a-d) show the morphology of CNTs synthesized on SS substrates subjected to chemical etching for 10, 20, 40, and 60 min, respectively. The insets show the corresponding top-view images of the CNTs. The growth was carried out at 600 °C for 10 min. The average diameter of CNTs for the case of 10 min etching was 190 nm and the length was 1.7 μm, see Fig. 3(a). The average length of the CNTs increased to 2.2 μm and 3.4 μm for CNTs synthesized on SS substrates subjected to the chemical etching for a period of 20 min and 40 min respectively, while the respective diameter decreased to 160 nm and 95 nm, see Fig. 3(b) and (c). The decrease in the diameter of the CNTs grown on SS for an increased etching time can be understood as follows: an increase in the etching period resulted in small catalyst particles on which CNTs with small diameter grew. A further increase in the chemical etching time to 60 min resulted in short and thick CNTs with a high degree of variation in the lengths. The average length of the resulting CNTs was 1.7 μm and the diameter was 140 nm, see Fig. 3(d). The chemical etching for 60 min resulted in rougher surface and reduced the density of small particles suitable for the nucleation and growth of the CNTs. Hence the site density of the CNTs decreased as evident from the top-view image in the inset of Fig. 3(d). A careful comparison between Figs. 1(b) and 3 (c) shows that, for the same growth time interval, the diameter and length were more uniform for the CNTs growth on chemically etched SS than that on the pristine SS substrate. An optimum chemical etching to the SS substrate induced a homogenous distribution of catalyst particles and resulted in the CNTs with uniform length and diameter. It is also noteworthy that generally the diameter of the CNTs synthesized on chemically etched SS is larger than the diameter of CNTs on pristine SS substrate. This result may indicate that, as compared to the catalyst nanoparticles from chemical etching method, smaller catalyst nanoparticles could be formed on the pristine SS substrate surface due to the NH_3 etching at 600

°C before the carbon precursor (C_2H_2) is introduced. These smaller catalyst nanoparticles will grow CNTs with smaller diameter. It should be noted that the CNTs grown on the SS substrate after 40 min etching have comparable diameter (95 nm) to that of the CNTs grown on pristine SS substrate (80 nm).

3.3 TEM analysis

The graphitic structures of the as-synthesized CNTs were verified by TEM analysis. Figs. 4(a) and 4(b) show the TEM images of the CNTs synthesized on pristine SS and Ni/Cr/SS substrates, respectively. The Ni thin layer acts as catalyst and Cr layer will ensure the better adhesion between the substrate and the as-synthesized CNTs [6]. The synthesis time was 10 minutes with the temperature maintained at 600 °C for both samples. TEM images show that there is a slight variation in the diameter of individual CNTs as the diameter is dependent on the size of the catalyst particle formed right before the introduction of C_2H_2. Big catalyst fragments result in thick tubes while small particles result in thin tubes. We found that both of these CNTs show similar growth mechanism with catalyst particles in the tip. The graphitic planes are not always parallel to the tube axis but are often twisted and broken to form a bamboo-like growth pattern, which is the common characteristic of the CNTs synthesized by PECVD process [21]. The inset on the left side of Fig. 4(a) shows a typical image of a catalyst rod encapsulated inside a CNT forming a core-shell structure. The compressive force of the graphene layers during the growth period results in the formation of these core-shell structures [22]. At nanoscale dimensions, the melting point of metal catalysts can be significantly lower than that of their bulk counterparts. Hence there is a high probability that the catalyst particles will be melted and trapped in the nanotubes. The HRTEM image, as shown in the inset on the right side of Fig. 4(a), shows the interface between the graphitic planes of CNTs and the planes of the catalyst core in the core-

shell structure. The graphitic planes of the CNT are observed on the right part of the image in light contrast. The catalyst core also exhibits crystalline structure with atomic plane separated by 0.21 nm corresponding to the Fe (111) planes. In most cases, the (111) lattice planes of Fe make an angle with the tube axis of CNTs. The concentric rings obtained in the selected area diffraction (SAED) pattern (inset in Fig. 4(b)) also confirm the graphitic structure of the CNTs. SAED pattern (not shown here) of the CNTs grown on pristine SS is similar to that in Fig. 4(b). The CNTs can have tapered (Fig. 4a) or cylindrical (Fig. 4b) tips depending on the plasma intensity during the CNT growth.

3.4 Field emission properties of CNTs

To understand the performance of CNT emitters, field emission current from CNTs synthesized on pristine SS was measured. The emission current was also compared with that of the CNTs synthesized on Ni/Cr coated SS as Cr is known to provide a stable adhesion of CNTs to the substrate. The synthesis time and temperature for the two CNT samples were 10 min 600 °C respectively. From the SEM images, the average length and diameter of the CNT emitters synthesized on the Ni/Cr coated SS are 2.8 μm and 100 nm respectively as shown in Fig. 5(a). The CNT emitters synthesized on pristine SS is similar to that in Fig. 1(b) with the diameter of 80nm and the average length of 3.4 μm. During the emission current measurement, the applied voltage was increased steadily in steps of 200 V until the emission current saturated. The emission current was increased to the maximum value for each sample and the applied voltage was kept constant for 15 h to test the stability of the emission current. The emission current was measured several times for each of the CNT samples exposed to the 'electric annealing' to confirm the repeatability of the emission characteristics. The field emission performance of the

CNTs synthesized on pristine SS and Ni/Cr coated SS is shown in Figs. 5(b-d). Both CNT emitters exhibited excellent field emission properties with high current density and long stability. From the curves of current density versus applied electric field (F-J plots) in Fig. 5(c), we can estimate the turn-on ($E_{turn-on}$) and threshold (E_{th}) electric fields. We define the $E_{turn-on}$ as the electric field required to obtain the emission current density of 1 $\mu A\ cm^{-2}$ and the E_{th} as the electric field required to obtain the emission current density of 1 $mA\ cm^{-2}$ [23]. The numerical values for $E_{turn-on}$ and E_{th} for CNTs on pristine SS were 4.7 V/μm and 8.3 V/μm, respectively. The $E_{turn-on}$ and E_{th} for the CNTs synthesized on Ni/Cr coated SS were 5.5 V/μm and 10 V/μm respectively. The lower values of $E_{turn-on}$ and E_{th} for the CNTs grown on pristine SS suggest that the electrons emission is easier from the CNTs grown on pristine SS substrate than from the CNTs grown on the Cr buffer layer on the SS substrate. During the process of field emission, the electron should cross the interface between the substrate and the buffer layer (Cr), then pass through the CNTs, and finally emit into the vacuum. Although the presence of a Cr layer would improve the adhesion of the CNTs to the SS substrate, the emitted electrons are subjected to a higher electrical contact resistance, which result in high $E_{turn-on}$ and E_{th}. CNTs synthesized on pristine SS exhibited lower $E_{turn-on}$ and E_{th} since they experience lower contact resistance than the CNTs synthesized on SS with the buffer layer of Cr.

We have estimated the field enhancement factor (β) for the two CNT emitters by first taking the logarithm of the equation (i) and plotting the graph of ln (J/F^2) versus 1/F (which is called the Fowler-Nordheim (F-N) plot). Then, the linear section of the F-N plot is fitted to get its slope which is the enhancement factor. Figure 5(d) shows the corresponding F-N plots for the CNT emitters grown on SS and on Ni/Cr coated SS. The straight line in the high electric field region shows the quantum mechanical tunneling process [24]. From the F-N plots, the field

enhancement factor (β) was estimated to be 1140 and 950 for CNTs grown on pristine SS and Ni/Cr coated SS, respectively, assuming the work function for CNTs is 5 eV. It is noteworthy that the experimental β is greater than geometrical β (the ratio of length to radius) of the CNTs by an order of magnitude. These large discrepancies between the β estimated from the F–N plots and geometrical $\beta \approx 60$ indicate that there are other mechanisms, such as vacuum space charge effects, in addition to quantum tunneling, for the field emission process [7].

The stability of the emission current is an important factor to be considered for the real application of CNTs in the field emission devices. To test the stability, the emission current of the CNT emitters was held at a maximum value for duration of 15 h, see Fig. 5(b). We observed only a small degradation in the emission current from the CNTs subjected to such stringent conditions over a long period of time. It is observed that the emission current from CNT emitters on Ni/Cr coated SS remained at a steady level over a long period of time during the stability tests. However, the current from CNT emitters on pristine SS deteriorated at a higher rate when the starting currents were held at the same level. Although the CNT emitters on pristine SS demonstrated greater field enhancement than the CNT emitters on Ni/Cr coated SS, the emission current of the CNT emitter on pristine SS is not as stable as that from the CNT emitter on the Ni/Cr coated SS. The deterioration of the current stability of the CNT emitters on pristine SS is attributed to the peel-off of the CNTs from the SS substrate by the electric field. The presence of the Cr buffer layer enhances the adhesion of CNTs to the substrate, as a result, the CNT emitters on Cr coated SS have a better stability.

The critical current, which is the maximum current that can be delivered through a single CNT before it breaks down, will increase with the diameter of the CNT. The critical current for

the CNTs with diameters in the range of 5-20 nm is 2-15 μA while the CNTs with diameter of about 30 nm can withstand a current of 40-250 μA [25]. The CNTs in the present work has diameter about 100 nm and are expected to withstand greater current without causing thermal degradation. Considering the density of the CNTs of 2×10^9 /cm^2 (estimated from the SEM images) and the emission current density of 1 mA/cm^2, the current per CNT is in the range of pA which is far below the critical current that a CNT can withstand. Therefore, the CNT emitters reported here have reasonably good stability. The above results show clearly that there is a trade-off between the emission properties (such $E_{turn\text{-}on}$ and E_{th}) and the stability if the Cr buffer layer is used. Further work is required to reveal the optimum thickness of the Cr layer so that it will not cause the increase in $E_{turn\text{-}on}$ and E_{th} while it can improve the stability of the CNT emitters.

4 Conclusions

In summary, vertically aligned CNTs have been synthesized on stainless steel substrates with or without chemical etching or catalyst deposition. The density and length of the CNTs are affected by the synthesis time. For a prolonged growth time, the catalyst activity is terminated and the plasma starts etching CNTs destructively. Chemical treatment to the substrate before the CNT synthesis has a profound effect on the diameter and length of the CNTs. CNTs with uniform diameter (95 nm) and length (3.4μm) have been synthesized on SS substrate chemically treated for 40 min. The CNTs synthesized on pristine SS substrates have demonstrated better field emission properties such as lower turn-on electric field, lower threshold electric field, and higher field enhancement while the CNTs synthesized on Ni/Cr coated SS have exhibited better electron emission stability. For practical application, a Cr buffer layer may be needed to coat the SS substrate to synthesize CNT emitters. However, the thickness of the Cr buffer layer needs to be

optimized to minimize the increase of the turn-on and threshold electric fields and meanwhile to improve the emission stability.

Acknowledgement

This work is supported by the National Science Foundation under grant 1043033 and the American Chemical Society under grant PRF# 51766-ND10. We are grateful to Dr. Gaohui Du for his help with the TEM experiment.

Figure captions:

Fig. 1. SEM images (30° tilt-view) of CNTs grown on pristine SS substrates at 600 °C for (a) 3 min, (b) 10 min, and (c) 20 min. The inset in each image shows the corresponding top-view images of the CNTs. All scale bars are 1 μm.

Fig. 2. AFM images of stainless steel substrates chemically etched for (a) 0, (b) 10, (c) 20, (d) 40, and (e) 60 min, respectively. (f) Graph showing the variation of surface roughness with different chemical etching time. The scan size of all AFM images is 1 μm.

Fig. 3. SEM images (30° tilt-view) of CNTs grown on SS substrates chemically etched in a mixture of H_2SO_4: H_2O_2: H_2O (4:1:15, volume ratio) for (a) 10 min, (b) 20 min, (c) 40 min, and (d) 60 min respectively. The synthesis was carried at 600 °C for 10 min. The insets show the corresponding top-view images of the CNTs. All scale bars are 1 μm.

Fig. 4. TEM images of CNTs synthesized on (a) pristine SS, and (b) Ni/Cr catalyzed SS. The inset on the left side of Fig. 4(a) shows a rod-like Fe catalyst encapsulated inside a CNT, forming a core-shell structure. The inset on the right side of Fig. 4(a) shows the interface between the graphitic layers of the CNT and the Fe trapped inside the CNT. The inset in Fig. 4(b) shows the SAED pattern of the CNTs and Fe-filled CNTs.

Fig. 5. Field emission properties of CNTs grown on pristine SS and Ni/Cr coated SS. (a) SEM images of CNT emitters on Ni/Cr coated SS (30° tilt-view), the CNTs were synthesized at 600 °C for 10 min. (b) Stability test, (c) F–J plots, and (d) Fowler–Nordheim (F–N) plots.

References

[1] S. Iijima, Nature 354 (1991) 56.

[2] W. A. Deheer, A. Chatelain, D. Ugarte, Science 270 (1995) 1179.

[3] Y. Wang, J. T. W. Yeow, J. Sensors 2009 (2009) 493904.

[4] S. H. Ng, J. Wang, Z. P. Guo, G. X. Wang, H. K. Liu, Electrochimica. Acta 51 (2005) 23.

[5] Z. F. Ren, Y. Lan, Y. Wang, In: P. Avouris, B. Bhusan, D. Bimberg, K. V. Klitzing, H. Sakaki, R. Wiesendenger (Eds.) Aligned Carbon Nanotubes: Nanoscience and Nanotechnology, Springer, Berlin, (2013), pp. 93-109.

[6] Y. Wang, J. Rybczynski, D. Z. Wang, K. Kempa, Z. F. Ren, W. Z. Li, B. Kimball, Appl. Phys. Lett 85 (2004) 4741.

[7] S. Neupane, M. Lastres, M. Chiarella, W. Z. Li, Q. M. Su, G. H. Du, Carbon 50 (2012) 2641.

[8] S. Talapatra, S. Kar, S. K. Pal, R. Vajtai, L. Ci, P. Victor, M. M. Shaijumon, S. Kaur, O. Nalamasu, P. M. Ajayan, Nat. Nanotechnol 1 (2006) 112.

[9] I. Lahiri, S. W. Oh, J. Y. Hwang, S. Cho, Y. K. Sun, R. Banerjee, W. Choi, ACS Nano 4 (2010) 3440.

[10] D. Q. Duy, H. S. Kim, D. M. Yoon, K. J. Lee, J. W. Ha, Y. G. Hwang, C. H. Lee, T. C. Bach, Appl. Surf. Sci 256 (2009) 1065.

[11] P. M. Parthangal, R. E. Cavicchi, M. R. Zachariah, Nanotechnology, 18 (2007) 185605.

[12] N. Wang, B. D. Yao, Appl. Phys. Lett 78 (2001) 4028.

[13] D. Park, Y. H. Kim, J. K. Lee, Carbon, 41 (2003) 1025.

[14] C. L. Lin, C. F. Chen, S. C. Shi, Diam. Relat. Mater 13 (2004) 1026.

[15] C. Masarapu, B. Q. Wei, Langmuir, 23 (2007) 9046.

[16] C. E. Baddour, F. Fadlallah, D. Nasuhoglu, R. Mitra, L. Vandsburger, J. L. Meunier, Carbon, 47 (2009) 313.

[17] M. D. Abad, J. C. S.Lopez, A. B. Murcia, V. B. Golovko, M. Cantoro, A.E.H. Wheatley, A. Fernandez, B.F.G. Johnson, J. Robertson, Diam. Relat. Mater 17 (2008) 1853.

[18] B. Kim, H. Chung, K. S. Chu, H. G. Yoon, C. J. Lee, W. Kim, Synth. Met 160 (2010) 584.

[19] G. Chen, S. Neupane, W. Li, L. Chen, J. Zhang, Carbon, 52 (2013) 468.

[20] C. Bower, O. Zhou, W. Zhu, D. J. Werder, S. H. Jin, Appl. Phys. Lett 77 (2000) 2767.

[21] M. Chhowalla, C. Ducati, N. L. Rupesinghe, K. B. K. Teo, G. A. J. Amaratunga, Appl. Phys. Lett 79 (2001) 2079.

[22] P. Buffat, J. P. Borel, Phys. Rev. A 13 (1976) 2287.

[23] G. H. Chen, D. H. Shin, T. Iwasaki, H. Kawarada, C. J. Lee, Nanotechnology 19 (2008) 415703.

[24] A. Pandey, A. Prasad, J. P. Moscatello, Y. K. Yap, ACS Nano 4 (2010) 6760.

[25] M. Doytcheva, M. Kaiser, N. de Jonge, Nanotechnology 17 (2006) 3226.

Figure 1

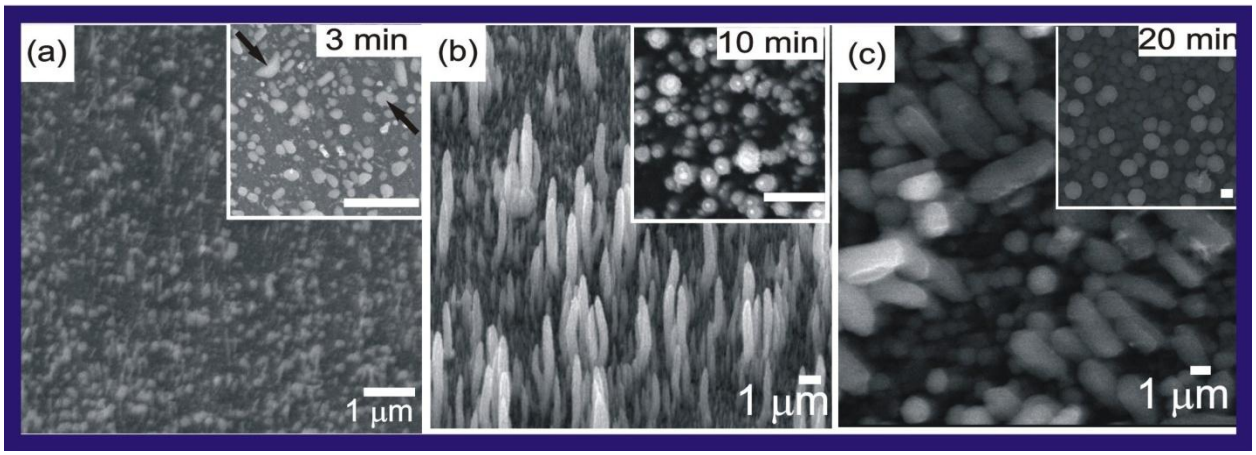

Figure 2

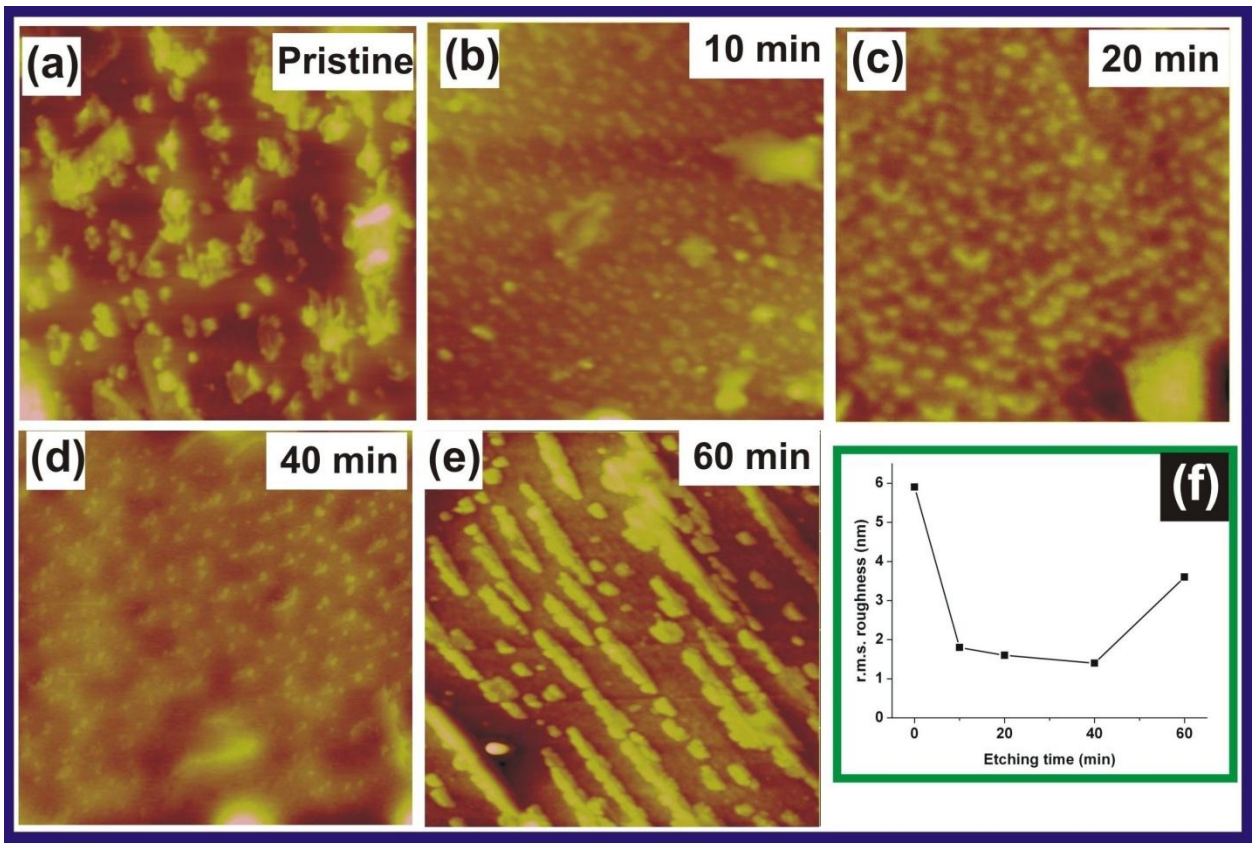
(a)
Pristine
(b)
10 min
(c)
20 min
(d)
40 min
(e)
60 min
(f)
r.m.s. roughness (nm)
0
1
2
3
4
5
6
0
20
40
60
Etching time (min)

Figure 3

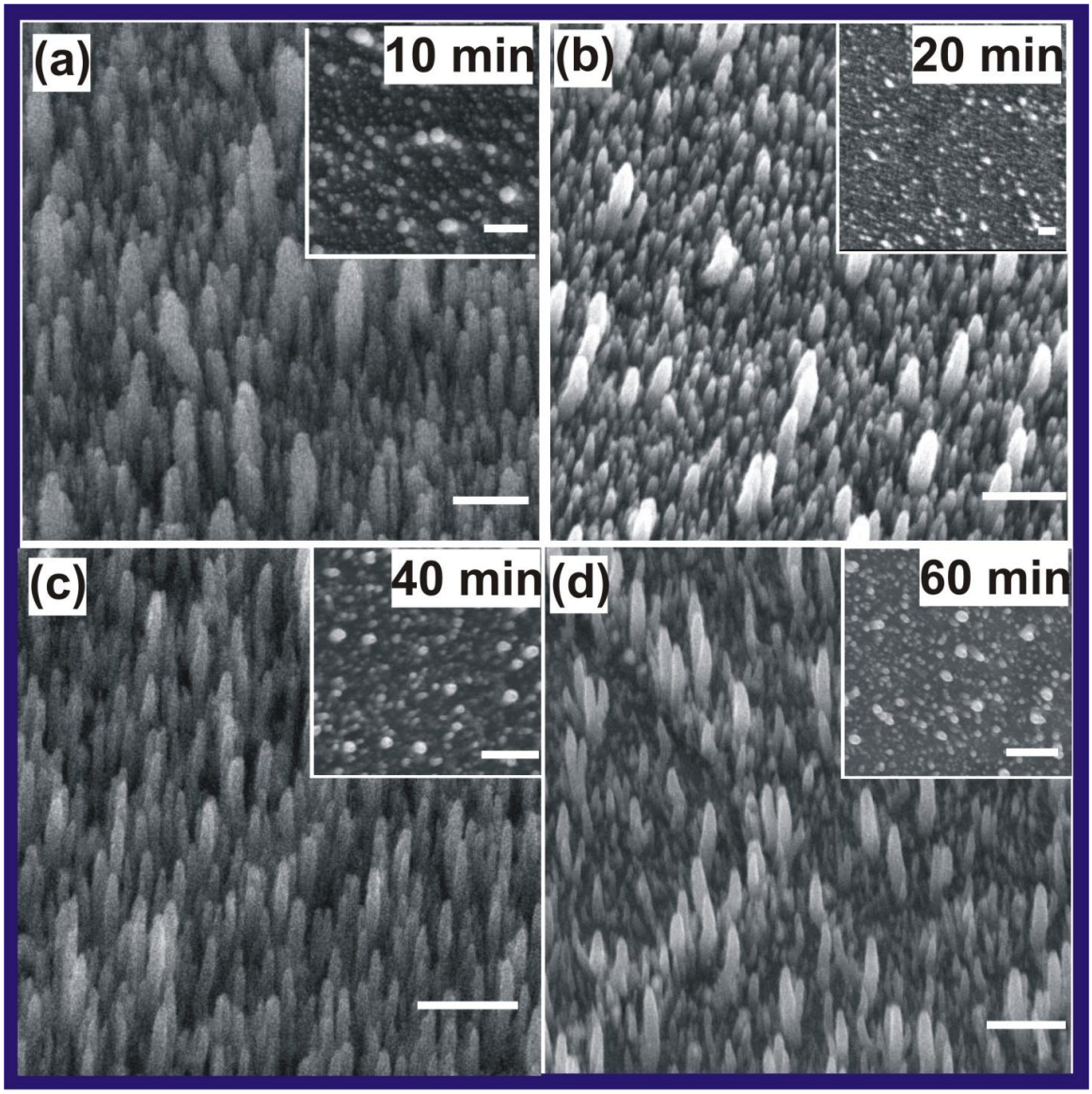

Figure 4

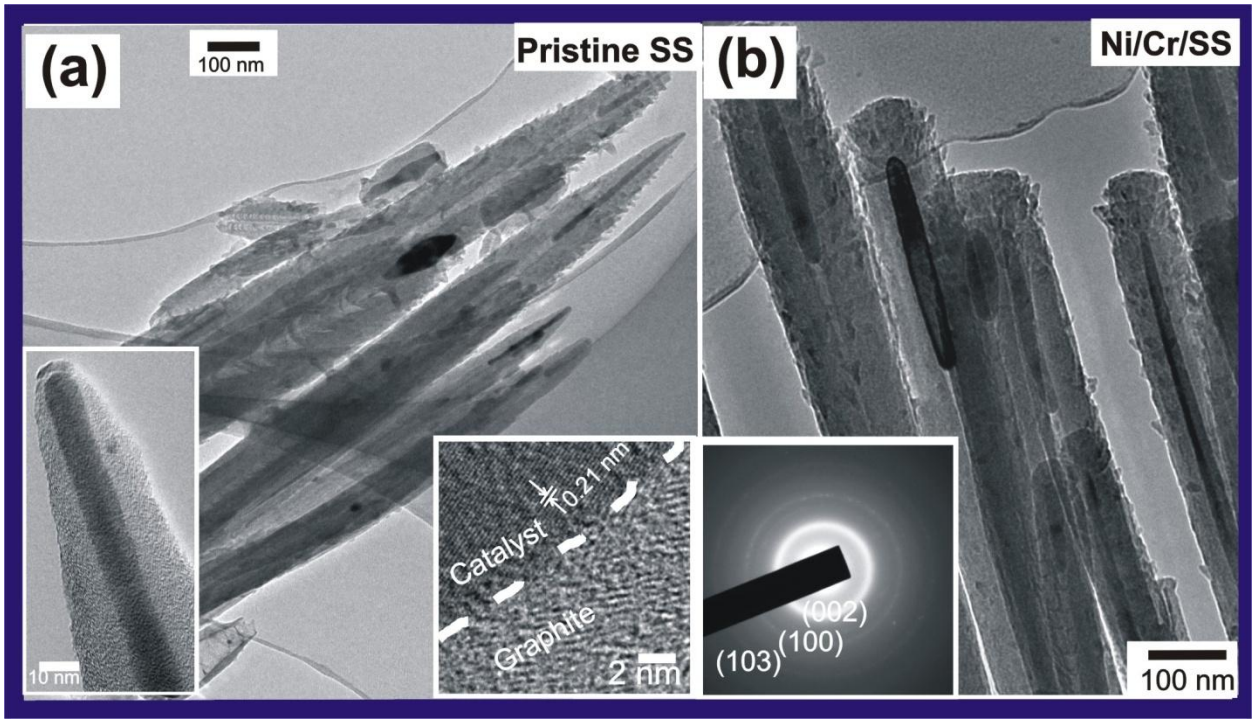
(a)
100 nm
Pristine SS
10 nm
Catalyst
0.21 nm
Graphite
2 nm
(b)
Ni/Cr/SS
(002)
(100)
(103)
100 nm

Figure 5

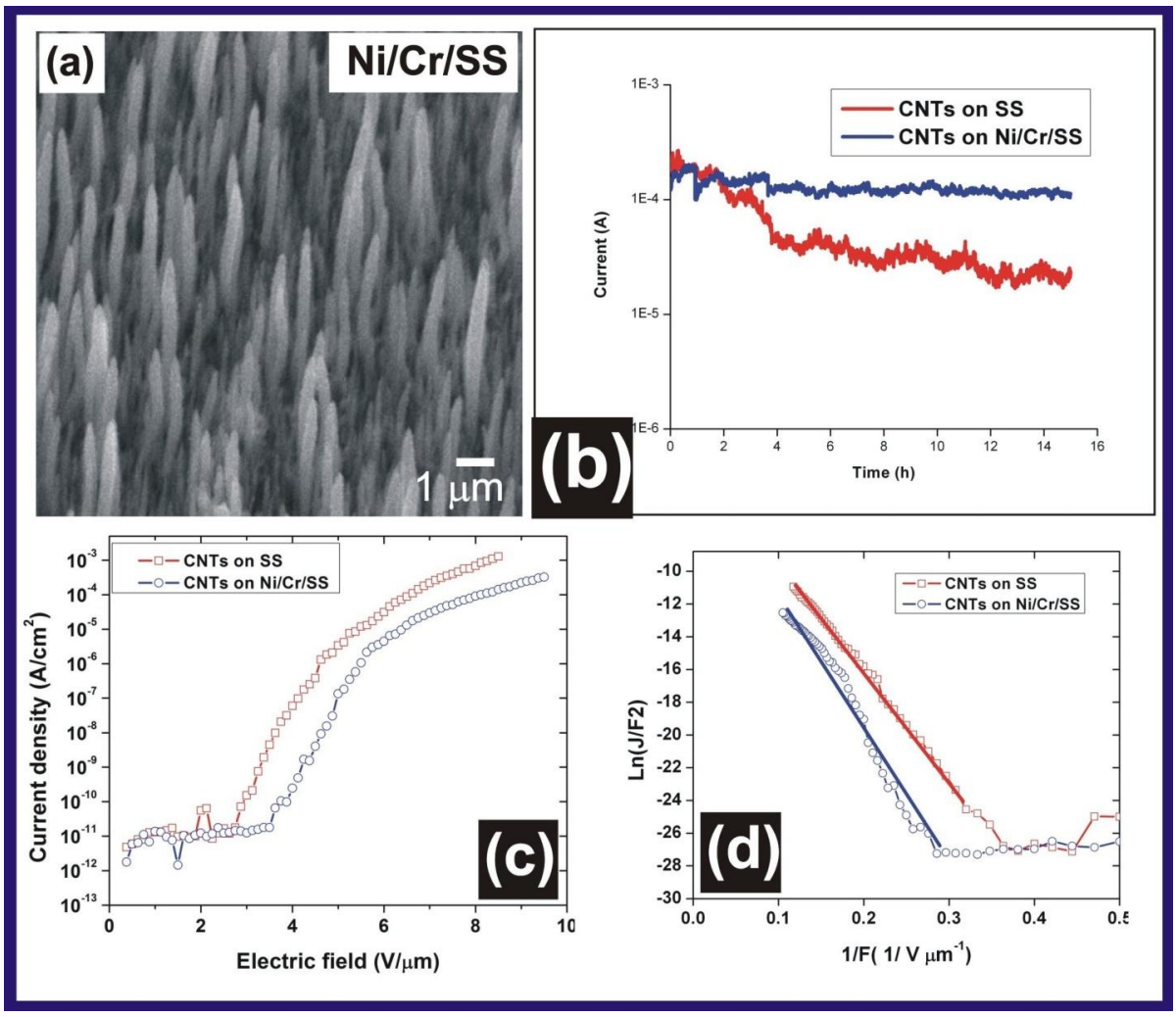
(a)
Ni/Cr/SS
1 μm
(b)
CNTs on SS
CNTs on Ni/Cr/SS
Current (A)
Time (h)
(c)
CNTs on SS
CNTs on Ni/Cr/SS
Current density (A/cm²)
Electric field (V/μm)
(d)
CNTs on SS
CNTs on Ni/Cr/SS
Ln(J/F2)
1/F(1/ V μm⁻¹)